

# Enhanced sensitivity for the detection of trace gases using multiple line integrated absorption spectroscopy

Andreas Karpf and Gottipaty N. Rao\*

Department of Physics, Adelphi University, Garden City, New York 11530, USA

\*Corresponding author: rao@adelphi.edu

Received 6 May 2009; revised 3 August 2009; accepted 21 August 2009;  
posted 24 August 2009 (Doc. ID 111007); published 10 September 2009

We describe a technique that enhances the sensitivity of a spectrometer for trace gas detection employing an external cavity continuously tunable CW quantum cascade laser and integrating the absorption spectra across multiple lines of the species. We demonstrate the power of this method by continuously recording the absorption spectra of NO<sub>2</sub> across the R branch from 1628.8 to 1634.5 cm<sup>-1</sup>. By integrating the resulting spectra, the detection sensitivity of NO<sub>2</sub> is improved by a factor of 15 compared to the sensitivity achieved using single line laser absorption spectroscopy with the same apparatus. This procedure offers much shorter data acquisition times for the real-time monitoring of trace gas species compared to adding repeated scans of the spectra to improve the signal-to-noise ratio. © 2009 Optical Society of America

OCIS codes: 000.2170, 010.1120, 120.6200, 280.3420, 300.1030, 300.6340.

## 1. Introduction

The precise monitoring of trace gases has applications in a wide range of fields, including the detection of environmental pollutants, tracking of contaminants in closed environmental systems, medical diagnostics, defense, and homeland security. In particular, real-time trace gas detection is important in environmental science (e.g., in atmospheric physics/chemistry concerning air quality control, for complying with Environmental Protection Agency (EPA) air quality regulations [1], safety monitoring, as well as for the study of chemical reactions that environmental gases (such as NO<sub>2</sub>) undergo, particularly in the presence of solar radiation). In these applications the concentrations of pollutants typically range from parts-per-million (ppm) to parts-per-trillion levels and thus require techniques that are both highly sensitive and selective. Nitrogen oxides (NO<sub>x</sub>) are some of the more damaging of these pollutants and impact the environment and public health in multiple ways.

They play important roles in the formation of photochemical smog, tropospheric ozone, and acid rain.

Laser-based techniques for monitoring environmental pollutants in the air have many advantages over chemical and other techniques because of their ability to provide real-time monitoring capabilities with greater sensitivity and selectivity. In particular, the advent of quantum cascade lasers in the mid-infrared region covering the 4–24 μm range has provided an attractive source for investigating the spectroscopy of trace gases in the atmosphere and for constructing portable gas sensors [2]. Quantum cascade lasers provide access to the fundamental rotational-vibrational transitions of molecular species [3], thus offering improved sensitivity of several orders of magnitude over near-infrared diode laser-based techniques that employ the detection of the overtones of these transitions. Quantum cascade lasers have been used to detect several trace gasses (e.g., CO, CO<sub>2</sub>, NO, NH<sub>3</sub>, CH<sub>4</sub>, and N<sub>2</sub>O) with different spectroscopic techniques (e.g., laser absorption spectroscopy, cavity ringdown spectroscopy, integrated cavity output spectroscopy) as described in

the review article by Tittel *et al.* [3]. By employing an external cavity arrangement, a quantum cascade laser offers a narrow linewidth ( $\Delta\nu \sim 0.001 \text{ cm}^{-1}$ ), highly stable and reproducible tunable CW output, and a wide continuous tuning range; all of which are essential for the study of complex spectra, as is the case in investigating trace gas components in the atmosphere [4,5].

Laser absorption spectroscopy is based on recording the change in intensity of laser radiation as it passes through a region containing the sample of interest. As the laser is tuned across a transition, the transmitted laser intensity is a function of frequency  $\nu$  given by Beer's law:

$$I(\nu) = I_0(\nu)e^{-\sigma(\nu)LN}, \quad (1)$$

where  $I_0$  is the incident laser intensity,  $L$  is the optical path length,  $\sigma(\nu)$  is the absorption coefficient, and  $N$  is the concentration of the absorbing species in molecules per unit volume [6]. The absorbance of the species in the cell is defined by  $a = \sigma(\nu)LN$ , and the maximum value of the absorbance of a line corresponds to  $a_{\text{max}}$ .

The sensitivity of a spectrometer is often determined by taking the ratio of the amplitudes of the absorption line to that of the noise level. As a result, it is important to maintain the sample at a pressure that results in a narrow linewidth and large amplitude. Maintaining the sample at low pressure reduces collisional broadening. At high pressures, neighboring lines tend to overlap because of collisional broadening. For example, the FWHM of the strongest  $\text{NO}_2$  transitions in the R branch ( $\nu \sim 1630 \text{ cm}^{-1}$ ) at atmospheric pressure are  $\sim 0.15 \text{ cm}^{-1}$  [7], which is much greater than the separation between the individual lines. It has been found that the optimal pressure for laser absorption techniques, such as tunable diode laser absorption spectroscopy (TDLAS), is in the 10–50 mbar range, which provides the best balance between sensitivity and selectivity [8]. Standard techniques, such as adding multiple scans, may be used to enhance the signal-to-noise ratio.

Using a line's amplitude to detect a species, however, neglects the width of the line and as a result gives the same intensity for both broad and narrow lines with the same amplitude [8]. This can be seen in Fig. 1, which shows a simulated  $\text{NO}_2$  absorption spectrum at pressures of 50, 200, and 600 mbars (the simulation was generated using the HITRAN database [7] and the SPECTRA software developed by Mikhailenko *et al.* [9]). Here we see that, even though the 600 mbar spectrum represents the contribution of about 12 times more molecules than the 50 mbar spectrum, it shows only about a 25% enhancement in peak absorption: The majority of additional absorption manifests itself in the broadening of the lines. It is important to note, however, that due to the closely spaced and complex nature of the  $\text{NO}_2$  spectrum, the individual absorption features seen in the 50 mbar trace are not individual absorption lines,

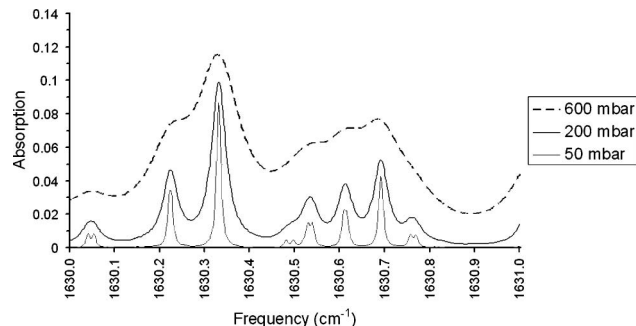


Fig. 1. Simulated  $\text{NO}_2$  absorption spectrum for a 25 ppm sample at pressures of 600, 200, and 50 mbars. The low-pressure data are helpful to resolve closely spaced lines.

but instead are composed of closely spaced doublets or multiplets. For example, the absorption feature seen at  $1630.23 \text{ cm}^{-1}$  is actually comprised of two lines separated by  $0.004 \text{ cm}^{-1}$  resulting from the transitions between the  $(0\ 0\ 1)-(18\ 2\ 17)$  and  $(0\ 0\ 0)-(17\ 2\ 16)$  levels (note that the  $(\nu_1\ \nu_3\ \nu_3)-(N\ K_a\ K_c)$  level notation is used) [7]. Even though the different rotational–vibrational transitions are not resolved, the absorption features that comprise several transitions can be employed for the estimation of trace species.

When dealing with broadened lines, a more accurate measure of the absorption intensity can be achieved by integrating over the absorption line. Assuming that the absorbance  $a = \sigma(\nu)LN$  is small (as is typically the case with trace gas detection), the integrated absorption may be written as

$$S = \int \sigma(\nu)NLd\nu. \quad (2)$$

If the separation between neighboring lines is much greater than the linewidth, the result of this integral may be used to obtain the actual concentration of molecules in the cell. If, on the other hand, the lines are closely spaced such that the observed spectra are the result of many overlapping lines, the direct retrieval of the concentration using Eq. (2) may not be practical.

The intensity of each of the rotational–vibrational transitions depends on a number of factors, such as the Einstein coefficients and energies of the transitions. However in the low concentration limit, the sum of the areas of a set of absorption lines varies linearly with the concentration. We define this sum  $S_T$  as a new experimental parameter and measure it for different concentrations of the target species. As a result, by using precalibrated reference mixtures of the desired gas, one can define an  $S_T$  versus concentration curve that characterizes a particular experimental apparatus (e.g., this would take into account the optical path length  $L$ , the tuning range, and other equipment-related factors). One could then identify the unknown concentrations of the species by recording their  $S_T$  and identifying their corresponding positions on this chart.

This procedure should enhance the sensitivity of detection in two ways. The first enhancement would be due to the summing of the area under many spectral lines (which would boost the magnitude of the recorded signal). The second enhancement is from the fact that the integration has the effect of averaging the random components of the noise. Because of the fact that this data is acquired in a single scan (which can take 1 s or less), this effective averaging of the noise occurs in a much shorter time span than would be the case for averaging the signal by adding repeated scans. The sensitivity is further enhanced over standard laser absorption techniques in that one is not limited to working in the low-pressure regime (i.e., there is no need to resolve the lines individually). One need only work in a pressure regime that is appropriate to identify the spectra of the species unambiguously. This procedure is particularly valuable for molecules that have a large number of transitions grouped together.

## 2. Experimental Details

We carried out absorption spectroscopy of  $\text{NO}_2$  using a short-path absorption cell (12.5 cm) filled with different concentrations of  $\text{NO}_2$  (25, 5, 2.5, 1, 0.5, and 0.25 ppm). The schematic of the experimental arrangement is shown in Fig. 2. Two, rectangular, flat, protected gold mirrors were aligned to reflect the beam back and forth seven times through the cell creating a homemade multipass cell that increased the path length to 0.88 m. The signal was detected using a two-stage, TE-cooled, IR photovoltaic detector (PVI-2TE-8 manufactured by Vigo), which can be operated in a room-temperature environment. The detectors were optically immersed in a high-refractive index, hyperhemispherical lens. Phase-sensitive detection was done using a chopper running at 3.9 kHz, and a lock-in amplifier (Stanford Research Systems SR830 DSP) with the time constant set to 1 ms.

The  $\text{NO}_2$  mixtures were prepared by loading the experimental cell with a precalibrated mixture of  $\text{NO}_2$  in zero air (a mix of 20.9%  $\text{O}_2$  and 79.1%  $\text{N}_2$ ). The  $\text{NO}_2$  mixtures were at concentrations of 25

and 5 ppm and were certified by Gasco Affiliates, LLC to  $\pm 10\%$  of the specified concentration. Other concentrations used in the experiment were created by loading the cell with the 5 ppm mixture to a certain pressure, and then adding zero air to increase the pressure to the desired final value. For example, the 1 ppm concentration was generated by first loading the experimental cell with  $120 \pm 10$  mbars of the precalibrated 5 ppm mix of  $\text{NO}_2$  before additional zero air was added to reach a final pressure of  $600 \pm 30$  mbars. Because of limitations in the accuracy of our vacuum/mixing apparatus, the concentrations prepared are expected to be accurate to  $\pm 30\%$  (e.g., the 2.5 ppm concentration mixture is expected to contain between 1.75 and 3.25 ppm  $\text{NO}_2$ ). For lower concentrations, the uncertainty rose to  $\pm 40\%$  for 0.5 and 0.25 ppm. The mixing apparatus was tested by generating several concentrations of  $\text{NO}_2$  and comparing the recorded absorption line intensities with the calculated intensities based on HITRAN [7]. This confirmed that the mixtures were within the expected uncertainty.

Experiments in the mid and far-infrared typically suffer from significant etalon effects. We identified etaloning in our signal due to a beam splitter. The etalon effects from the beam splitter were removed by placing it between the lenses of a  $2\times$  beam expander ( $f_1 = 25.8$  mm,  $f_2 = 50.6$  mm); the short focal lengths were necessary to create enough divergence to remove the etalon peaks. Wedge windows (AR coated ZnSe with faces that were  $1^\circ$  away from parallel) were used in the cell to remove etaloning that occurs with standard, parallel-faced windows. The quantum cascade laser itself exhibited etaloning due to its antireflection coatings. We compensated for this by subtracting empty-cell scans of the laser (which characterized the tuning characteristics of the laser including etaloning) from scans of the cell loaded with  $\text{NO}_2$ .

The quantum cascade laser source was purchased from Daylight Solutions (Model TLS-CW-MHF) and has a tuning range of  $1601.3$  to  $1670$   $\text{cm}^{-1}$ . The external cavity is of Littrow configuration, which allows a wide range of mode-hop free tuning, provides a narrow linewidth ( $\sim 0.001$   $\text{cm}^{-1}$ ), and is thus well suited for spectroscopic measurements. The laser tuning was monitored using an etalon and the laser controller's display screen, as well as by comparing recorded spectra with line positions identified in the HITRAN database [7]. The laser power varies as a function of tuning, with a minimum output power of 14 mW at  $1601.3$   $\text{cm}^{-1}$ , and a maximum of 21 mW at  $1640.4$   $\text{cm}^{-1}$ . The output power at  $1630$   $\text{cm}^{-1}$  (the frequency at which we conducted laser absorption spectroscopy) was 19.5 mW. Broad range tuning is achieved entirely by rotating the external cavity grating via a stepper motor; no current or temperature tuning was necessary. The system may be set to one of six preset tuning rates, the slowest of which was  $3.125$   $\text{cm}^{-1}/\text{s}$  (the tuning rate used to record

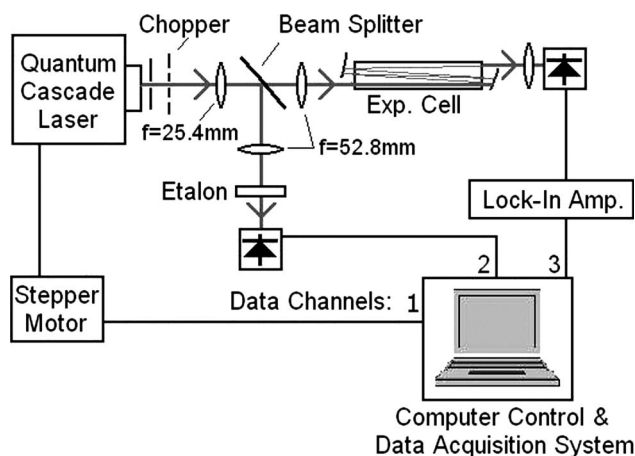


Fig. 2. Experimental apparatus used for absorption spectroscopy of  $\text{NO}_2$ .

our NO<sub>2</sub> absorption spectra). The minimum spot size of the beam is approximately 2 mm.

To integrate the recorded spectra for multiple lines over a desired range of frequencies, the laser source must tune without mode hops across that range. The quantum cascade laser used in this experiment was capable of mode-hop free tuning between 1603.5 and 1670 cm<sup>-1</sup>. This provided access to half of the NO<sub>2</sub> P branch and the entire NO<sub>2</sub> R branch (the peak absorption in the R branch occurs at 1630.3 cm<sup>-1</sup>). The next consideration was to select a region with a strong dense spectrum and which was free from interference due to water lines. Figure 3(a) shows a simulated spectrum illustrating the regions where the water lines (due to ambient water vapor in the beam path leading to the experimental cell) overlap and thus overwhelm any potential signal from the NO<sub>2</sub> R branch. As described before, this simulation was generated using the HITRAN database [7] and the SPECTRA software developed by Mikhailenko *et al.* [9]. The strength of the water lines was selected to match typical conditions in the midlatitude U.S. during the summer months (the water vapor density used was 14.97 g/m<sup>3</sup>, which corresponds to a relative humidity of 71% at 23 °C, and is the average humidity in Washington D.C. in July) [10]. As is seen in the figure, the region between the water lines at 1627.82 and 1634.97 cm<sup>-1</sup> proves to be the longest continuous region in which absorption due to the water lines does not overwhelm the NO<sub>2</sub> lines, and covers the peak of the R branch. Because of the broad width of these water lines, our ability to record NO<sub>2</sub> spectra was limited to the region between 1628.8 and 1634.5 cm<sup>-1</sup>. It is important to note that this tuning range covered over 500 NO<sub>2</sub> transitions, of which approximately 20% may be considered relatively strong (i.e., having transition strengths over 10% that of the strongest transition in the R branch). It should also be noted that the strength and width of the water lines in the simulation were calibrated to match our experimental apparatus (which had a 1 m path from the laser to the experimental cell).

To facilitate the analysis, the NO<sub>2</sub> concentrations were maintained at a pressure of 600 ± 30 mbars. This narrowed the linewidth enough so that we were able to determine the frequency at which the interference from the water lines prevented the accurate recording of NO<sub>2</sub> spectra. The data were recorded by reading the output from the Vigo detectors into a PC using a National Instruments (model PCI-6040E) data acquisition board. A virtual instrument constructed using LabView for Windows was used to record the data.

### 3. Results and Discussion

Absorption spectra were recorded for several concentrations of NO<sub>2</sub>: 25, 12.5, 5, 2.5, 1, 0.5, 0.25, and 0 ppm. The 0 ppm spectrum was recorded to determine the noise contributions from all components of the experiment as well as the contributions from the tails of the water lines in the region of interest

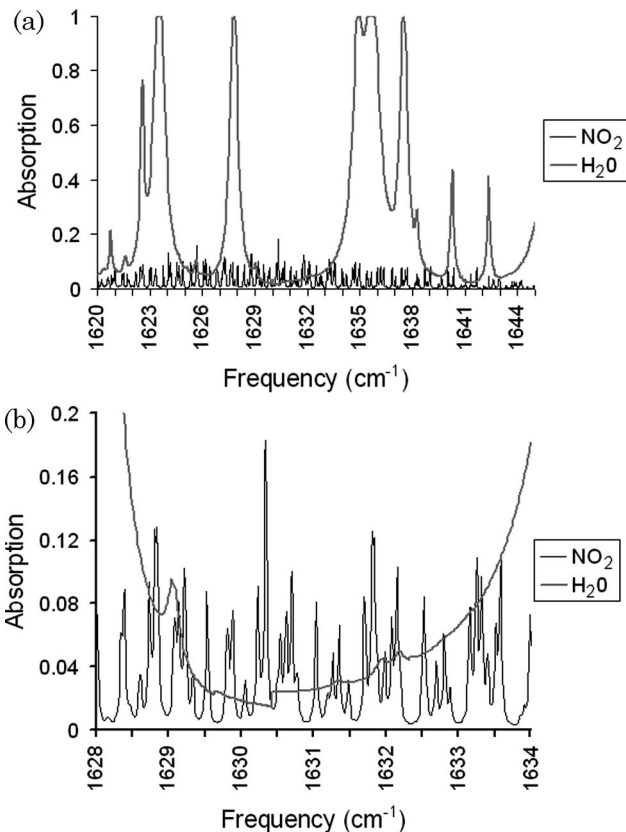


Fig. 3. (a) Simulated NO<sub>2</sub> spectrum (50 ppm at 200 mbars) for the R branch between 1620 and 1645 cm<sup>-1</sup>. Overlaid onto the spectrum are the water lines that match typical conditions in the midlatitude U.S. during the summer months. This spectrum was used to select a region with a strong dense NO<sub>2</sub> spectrum that was free from interference due to water lines. (b) Close-up of the region whose spectrum was recorded and integrated.

and was generated by filling the sample cell with zero air. It should be stated that high-end estimates for the errors and uncertainties were used and therefore the improvement in the sensitivity of detection employing multiple line integrated absorption

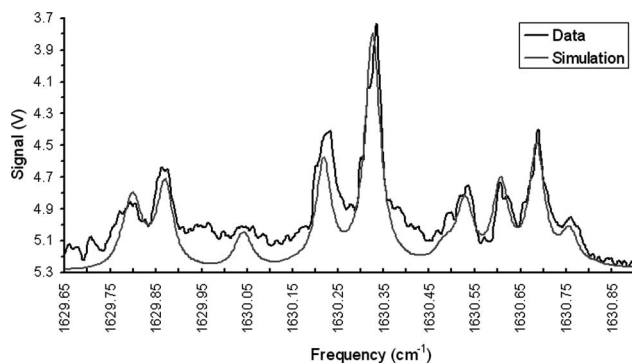


Fig. 4. Absorption spectrum of NO<sub>2</sub> (concentration = 25 ± 3 ppm, pressure = 200 ± 20 mbars) recorded from 1629.65 to 1630.95 cm<sup>-1</sup>. The strong absorption feature located at approximately 1630.33 cm<sup>-1</sup> was used to determine the sensitivity of the apparatus. This feature is comprised of two strong, closely spaced doublets (identified in Table 1). The gray trace is the simulated spectrum based on HITRAN data [7].

**Table 1. Spectral Line Parameters from HITRAN [7] for the Major NO<sub>2</sub> Doublets in the R Branch that Make Up the Absorption Feature at 1630.33 cm<sup>-1</sup><sup>a</sup>**

Central Frequency of Doublet (cm <sup>-1</sup> )	Upper State						Lower State					
	( $\nu_1$	$\nu_3$	$\nu_3$ )	( $N'$	$K'_a$	$K'_c$ )	( $\nu_1$	$\nu_3$	$\nu_3$ )	( $N''$	$K''_a$	$K''_c$ )
1630.326	(0	0	1)	(17	1	16)	(0	0	0)	(16	1	15)
1630.328	(0	0	1)	(17	0	17)	(0	0	0)	(16	0	16)

<sup>a</sup>As seen in Fig. 4.

spectroscopy reported later in this section is a conservative estimate.

We first determined the sensitivity of the apparatus using laser absorption spectroscopy by recording NO<sub>2</sub> spectra at concentrations of 25, 12.5, and 5 ppm (at a pressure of 200 ± 20 mbars) between 1629.65 and 1630.95 cm<sup>-1</sup> (Fig. 4 shows the spectrum recorded at a concentration of 25 ppm). The pressure was chosen to facilitate the identification and measurement of individual absorption features; the range was chosen because it allows the analysis of the strongest absorption feature in the R branch. This feature is located at approximately 1630.33 cm<sup>-1</sup> and is in fact comprised of two, closely spaced doublets. All four lines are grouped within 0.003 cm<sup>-1</sup>. This is narrower than the 0.04 cm<sup>-1</sup> FWHM of the individual lines at 200 mbars and results in the single observed absorption feature. The two doublets that form the feature are identified in Table 1. The observed amplitude of this absorption feature is plotted for each concentration in Fig. 5. A weighted linear least-squares fit of the data is then used to determine the sensitivity. We take the y-intercept value of 0.078 V and divide it by the slope of the fit (0.0432 V/ppm) to obtain a sensitivity of approximately 1.8 ppm.

To measure the sensitivity that may be obtained by integrating the multiline absorption spectra recorded over a tuning range, we recorded the absorption spectra for six concentrations of NO<sub>2</sub> (5, 2.5, 1, 0.5, 0.25, and 0 ppm), at a pressure of

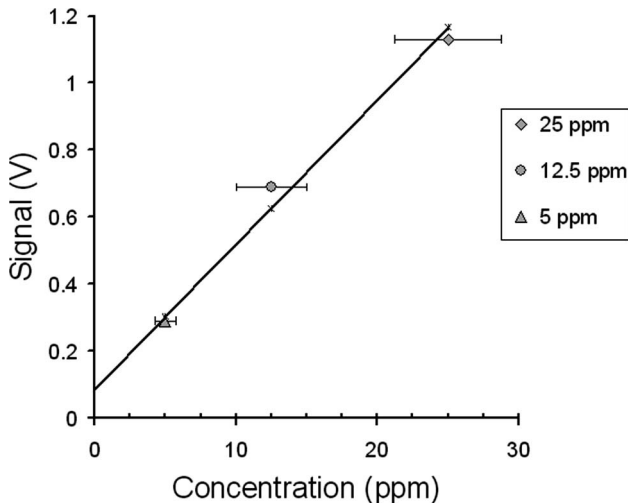


**Fig. 5.** Absorption signal intensity of NO<sub>2</sub> recorded at concentrations of 25, 12.5, and 5 ppm. The y intercept of the weighted least-squares fit of the data indicates the sensitivity of the apparatus.

600 ± 30 mbars. The spectra were recorded in the frequency range of 1628.8 to 1634.5 cm<sup>-1</sup>. These concentrations were selected to ensure that the data were in the weakly absorbing regime (i.e., the absorption of the strongest line was less than 5%). The data from each spectrum were then integrated to yield the total absorption strength  $S_T$  for the corresponding concentration. Each of these values is subtracted from the total absorption strength recorded for the 0 ppm concentration; this results in the area under the recorded absorption spectrum for the corresponding concentration (we refer to this as the total absorption signal for a given concentration). Figure 6 shows a plot of the total absorption signal versus concentration, as well as a weighted linear least-squares fit of this data (the y axis is given in arbitrary units).

The instrument's sensitivity is determined from the y intercept of the linear fit. We take the y-intercept value of 18.7 total absorption units and divide it by the slope of the fit (161 total absorption units/ppm) to obtain a sensitivity of approximately 120 ppb. This shows a factor of 15 improvement in sensitivity compared to laser absorption spectroscopy conducted using the same apparatus. One should note that even though the NO<sub>2</sub> mixtures were generated using zero air (a dehumidified air mixture), our results are representative of what one would expect if the NO<sub>2</sub> was in ambient air. This is a result of our experimental layout, where the laser beam travels through approximately 1 m of ambient air before reaching the cell whose effective path length is 88 cm.

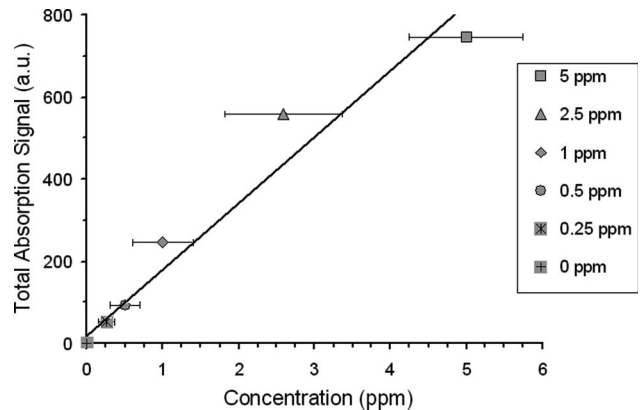


**Fig. 6.** Total absorption signal versus concentration plot. The expected linear relationship between the integrated absorption signal of the various concentrations is seen. The y intercept is used to determine the sensitivity of detection.

#### 4. Conclusion

We describe and demonstrate a technique which enhances the sensitivity of a spectrometer for trace gas detection by integrating the absorption spectra from multiple spectral lines. In particular, we use laser absorption spectroscopy with a tunable, CW quantum cascade laser, and a short-path absorption cell to detect low concentrations of NO<sub>2</sub> with a sensitivity of approximately 1.8 ppm. Employing the multiple line integrated absorption technique with the same experimental apparatus, we detect concentrations of NO<sub>2</sub> with a sensitivity on the order of 120 ppb, demonstrating a greater than 1 order of magnitude improvement in the instrument's sensitivity. We feel that this technique may be useful for detection of polyatomic species such as NO<sub>2</sub> that have dense rotational-vibrational spectra over a relatively compact frequency range. Though this experiment was conducted using a quantum cascade laser with a wide mode-hop free tuning range, it could be applied using any tunable laser source that is capable of tuning across multiple transitions of the target species. Additional improvements to the sensitivity may be achieved by using this technique with long optical path-length apparatus, such as a Herriot cell or ICOS, and should enable sub-ppb sensitivity.

#### References

1. United States Environmental Protection Agency, "National Air Quality Status and Trends Through 2007," EPA-454/R-08-006, United States Environmental Protection Agency, 2008.
2. A. A. Kosterev, R. F. Curl, F. K. Tittel, M. Rochat, M. Beck, D. Hofstetter, and J. Faist, "Chemical sensing with pulsed QC-DFB lasers operating at 6.6  $\mu\text{m}$ ," *Appl. Phys. B* **75**, 351–357 (2002).
3. F. K. Tittel, Y. Bakhirkin, A. Kosterev, and G. Wysocki, "Recent advances in trace gas detection using quantum and interband cascade lasers," *Rev. Laser Engin.* **34**, 275–282 (2006).
4. G. Wysocki, R. Curl, F. Tittel, R. Maulini, J. Billiard, and J. Faist, "Widely tunable mode-hop free external cavity quantum cascade laser for high resolution spectroscopic applications," *Appl. Phys. B* **81**, 769–777 (2005).
5. A. Karpf and G. N. Rao, "Absorption and wavelength modulation spectroscopy of NO<sub>2</sub> using a tunable, external cavity continuous wave quantum cascade laser," *Appl. Opt.* **48**, 408–413 (2009).
6. P. Werle, "A review of recent advances in semiconductor laser based gas monitors," *Spectrochim. Acta A* **54**, 197–236 (1998).
7. L. S. Rothman, D. Jacquemart, A. Barbe, D. Chris Benner, M. Birk, L. R. Brown, M. R. Carleer, C. Chackerian, Jr., K. Chance, L. H. Coudert, V. Dana, V. M. Devi, J.-M. Flaud, R. R. Gamache, A. Goldman, J.-M. Hartmann, K. W. Jucks, A. G. Maki, J.-Y. Mandin, S. T. Massie, J. Orphal, A. Perrin, C. P. Rinsland, M. A. H. Smith, J. Tennyson, R. N. Tolchenov, R. A. Toth, J. Vander Auwera, P. Varanasi, and G. Wagner, "The HITRAN 2004 molecular spectroscopic database," *J. Quant. Spectrosc. Radiat. Transfer* **96**, 139–204 (2005).
8. J. M. Hollas, *High Resolution Spectroscopy, Second Edition* (Wiley, 1998).
9. C. N. Mikhailenko, Yu. L. Babikov, and V. F. Golovko, "Information-calculating system spectroscopy of atmospheric gases. The structure and main functions," *Atmos. Oceanic Opt.* **18**, 685–695 (2005).
10. National Oceanic and Atmospheric Administration, "Average relative humidity," <http://lwf.ncdc.noaa.gov/oa/climate/online/ccd/avgrh.html>.